Dark-Sector Search via Pion-Produced η and η' Mesons Decaying Invisibly in the NA64h Detector

Yu. M. Andreev,[1] A. Antonov,[2] M. A. Ayala Torres,[3,4] D. Banerjee,[5] B. Banto Oberhauser,[6] J. Bernhard,[5] P. Bisio,[2,7] A. Celentano,[2] N. Charitonidis,[5] D. Cooke,[8] P. Crivelli,[6,*] E. Depero,[6] A. V. Dermenev,[1] S. V. Donskov,[1] R. R. Dusaev,[1] T. Enik,[9] V. N. Frolov,[9] S. V. Gertsenberger,[9] S. Girod,[5] S. N. Gninenko,[1,4,†] M. Hösgen,[10] V. A. Kachanov,[1] Y. Kambar,[9] A. E. Karneyeu,[1] G. D. Kekelidze,[9] B. Ketzer,[10] D. V. Kirpichnikov,[1] M. M. Kirsanov,[1] V. N. Kolosov,[1] V. A. Kramarenko,[1,9] L. V. Kravchuk,[1] N. V. Krasnikov,[1,9] S. V. Kuleshov,[3,4,‡] V. E. Lyubovitskij,[1,11,4] A. Marini,[2] L. Marsicano,[2] V. A. Matveev,[9] R. Mena Fredes,[4,11] R. G. Mena Yanssen,[4,11] L. Molina Bueno,[12] M. Mongillo,[6] D. V. Peshekhonov,[9] V. A. Polyakov,[1] B. Radics,[13] K. M. Salamatin,[9] V. D. Samoylenko,[1] H. Sieber,[6] D. A. Shchukin,[1] O. Soto,[14,4] V. O. Tikhomirov,[1] I. V. Tlisova,[1] A. N. Toropin,[1] M. Tuzi,[12] P. V. Volkov,[9] V. Yu. Volkov,[1,§] I. V. Voronchikhin,[1] J. Zamora-Saá,[3,4] and A. S. Zhevlakov[9]

(NA64 Collaboration)

[1]*Authors affiliated with an institute covered by a cooperation agreement with CERN*
[2]*INFN, Sezione di Genova, 16147 Genova, Italia*
[3]*Center for Theoretical and Experimental Particle Physics, Facultad de Ciencias Exactas, Universidad Andres Bello, Fernandez Concha 700, Santiago, Chile*
[4]*Millennium Institute for Subatomic Physics at High-Energy Frontier (SAPHIR), Fernandez Concha 700, Santiago, Chile*
[5]*CERN, European Organization for Nuclear Research, CH-1211 Geneva, Switzerland*
[6]*ETH Zürich, Institute for Particle Physics and Astrophysics, CH-8093 Zürich, Switzerland*
[7]*Università degli Studi di Genova, 16126 Genova, Italia*
[8]*UCL Departement of Physics and Astronomy, University College London, Gower St. London WC1E 6BT, United Kingdom*
[9]*Authors affiliated with an international laboratory covered by a cooperation agreement with CERN*
[10]*Universität Bonn, Helmholtz-Institut für Strahlen-und Kernphysik, 53115 Bonn, Germany*
[11]*Universidad Técnica Federico Santa María and CCTVal, 2390123 Valparaíso, Chile*
[12]*Instituto de Fisica Corpuscular (CSIC/UV), Carrer del Catedratic Jose Beltran Martinez, 2, 46980 Paterna, Valencia, Spain*
[13]*York University, Toronto, Canada*
[14]*Departamento de Fisica, Facultad de Ciencias, Universidad de La Serena, Avenida Cisternas 1200, La Serena, Chile*

(Received 6 June 2024; accepted 13 August 2024; published 20 September 2024; corrected 4 October 2024)

We present the first results from a proof-of-concept search for dark sectors via invisible decays of pseudoscalar η and η' mesons in the NA64h experiment at the CERN SPS. Our novel technique uses the charge-exchange reaction of 50 GeV π^- on nuclei of an active target as the source of neutral mesons. The $\eta, \eta' \to$ invisible events would exhibit themselves via a striking signature—the complete disappearance of the incoming beam energy in the detector. No evidence for such events has been found with 2.9×10^9 pions on target accumulated during one day of data taking. This allows us to set a stringent limit on the branching ratio $\mathrm{Br}(\eta' \to \text{invisible}) < 2.1 \times 10^{-4}$ improving the current bound by a factor of $\simeq 3$. We also set a limit on $\mathrm{Br}(\eta \to \text{invisible}) < 1.1 \times 10^{-4}$ comparable with the existing one. These results demonstrate the great potential of our approach and provide clear guidance on how to enhance and extend the sensitivity for dark sector physics from future searches for invisible neutral meson decays.

DOI: 10.1103/PhysRevLett.133.121803

[*]Contact author: paolo.crivelli@cern.ch
[†]Contact author: sergei.gninenko@cern.ch
[‡]Contact author: serguei.koulechov@cern.ch
[§]Deceased.

Decays of the pseudoscalar neutral mesons (M^0), such as $\pi^0, \eta, \eta', K_S^0, K_L^0$, provide a unique opportunity to probe new physics beyond the standard model (SM) [1]. Searching for their decay into invisible final states is particularly advantageous because in the SM the branching fraction of the M^0 decay into a neutrino-antineutrino pair, $\mathrm{Br}(M^0 \to \nu\bar{\nu})$, is predicted to be extremely small [2]. Indeed, for massless neutrinos, this transition is forbidden kinematically by angular momentum conservation. For the case of massive neutrinos, one of them is forced to be in a helicity-suppressed state resulting in $\mathrm{Br}(M^0 \to \nu\bar{\nu})$ to be proportional to the neutrino-meson mass ratio squared, $\sim m_\nu^2/m_{M^0}^2 \lesssim 10^{-16}$, for $m_\nu \lesssim 10$ eV and $m_{M^0} \simeq m_\eta \simeq 0.5$ GeV [1]. In the SM the helicity suppression can be overcome for the four-neutrino final state, however, in this case, $\mathrm{Br}(M^0 \to \nu\bar{\nu}\nu\bar{\nu}) \lesssim 10^{-18}$ [3]. Thus, if the decay $M^0 \to$ invisible is observed it would unambiguously signal the presence of new physics.

Various extensions of the SM could significantly enhance the invisible decay rate of η, η', and K_S^0, K_L^0 up to a measurable level, for a recent review see, e.g., Ref. [4], and Refs. [5–11], respectively. Some of the scenarios consider dark sector physics, including light dark matter (DM), with masses of the DM particles (χ) much below the electroweak scale, $m_\chi \ll \Lambda_{\mathrm{EW}} \simeq 100$ GeV, which has a new interaction between the SM and DM transmitted by a scalar mediator [12]. Such mediator naturally couples more strongly to DM than SM particles, hence it would dominantly decay invisibly if kinematically allowed. The $\eta^{(\prime)} \to$ invisible process could occur via the decay into pairs of mediators subsequently decaying to DM particles [12], or from direct decay $\eta^{(\prime)} \to \chi\chi$ [13,14]. An interesting case is when the (pseudo)scalar mediator is leptophobic, i.e., transmits interaction between the χ and light SM quarks, and can accommodate the relic DM density, see, e.g., [15,16]. Another attractive model considers the $\eta^{(\prime)} \to$ invisible decay into a pair of heavy neutrinos [17].

Searching for the $M^0 \to$ invisible decay is challenging, as it requires a combination of an intense source of M^0s and a well-defined high-purity signature to tag their production. The most sensitive limit, $\mathrm{Br}(M^0 \to \text{invisible}) \lesssim 10^{-9}$, is obtained for π^0's produced via the $K^- \to \pi^-\pi^0$ decay [18]. Several previous searches for $\eta, \eta' \to$ invisible decays have been performed at e^+e^- colliders by the BES [19], CLEO [20], and BESIII [21] experiments. However, the best upper limits $\mathrm{Br}(\eta \to \text{invisible}) < 1.0 \times 10^{-4}$ and $\mathrm{Br}(\eta' \to \text{invisible}) < 6.0 \times 10^{-4}$ at 90% confidence level (CL) obtained by BESIII, are still much less stringent compared to the π^0 one. These bounds were obtained from a sample of $\sim 2.3 \times 10^8$ J/ψ events collected during ~50 days of running at the BEPCII [22] by using $J/\psi \to \phi\eta, \phi\eta'$; $\phi \to K^+K^-$ decay chain as a source of tagged η, η' [21].

In this Letter, we report the first results of the search for invisible η, η' decays in the NA64h fixed-target active beam-dump experiment at the CERN Super Proton Synchrotron accelerator (SPS) [23,24] obtained from one day of data taking from a run with a hadron(h) beam. The method we chose for the search was proposed in Ref. [6]. The source of the η and η' mesons is the quasi-elastic charge exchange reaction of 50 GeV π^-'s on nuclei $A(Z)$ of an active target

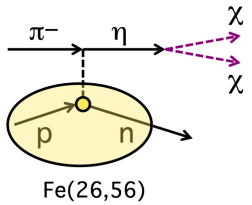

FIG. 1. Diagrams illustrating the η production in the quasielastic charge exchange reaction of Eq. (1).

$$\pi^- + A(Z) \to \eta^{(\prime)} + n + A(Z-1); \qquad \eta^{(\prime)} \to \text{invisible} \qquad (1)$$

as illustrated in Fig. 1. Here, the neutral meson is emitted mainly in the forward direction with the beam momentum and the recoil nucleon or nuclei carrying away a small fraction of the beam energy. The term "quasielastic reaction" as applied to the process (1) means that, unlike elastic reactions of charge exchange with the proton, the transition can occur for the target nucleus as a whole into an excited state followed by its fragmentation. Since the binding energy in the nucleus is a few MeV/nucleon, the velocity $v \sim q/\text{mass}$ of the daughter particles, where $q \lesssim 0.03$ GeV/c is the momentum transfer, is on average small. At high initial energies, the nucleus does not have time to collapse during the interaction (the characteristic transverse distances is $l \simeq 1/q$). After the collision, the nucleus disintegrates into fragments, which are absorbed into the target. Hence the experimental signature of the reaction (1), is an event with *full disappearance of the beam energy*. The decay $\eta^{(\prime)} \to$ invisible is expected to be a very rare event that occurs with a much smaller frequency than the $\eta^{(\prime)}$ production rate. Hence, its observation presents a challenge for the design and performance of the detector. However, despite a relatively small $\eta^{(\prime)}$ production rate the signature of the signal event (1) is very powerful allowing a strong background rejection.

The schematic of the NA64h detector modified for a sensitive search for the reaction (1) is shown in Fig. 2. The experiment employs the H4 50 GeV pion beam at the CERN SPS with intensity $\simeq 10^6$ π^- per SPS spill of 4.8 s [25]. The K^- contamination in the beam at the production target ($K^-/\pi^- \simeq 5 \times 10^{-2}$) is reduced to $\simeq 2.5 \times 10^{-2}$ at the detector location due to K^- decay in flight [26]. The beam is defined by the scintillator (Sc) counters S_{1-4}. A magnetic spectrometer (MBPL) is used to reconstruct the momentum of the incoming π^-'s with a precision $\delta p/p \simeq 1\%$ [27]. The spectrometer consists of two consecutive dipole magnets

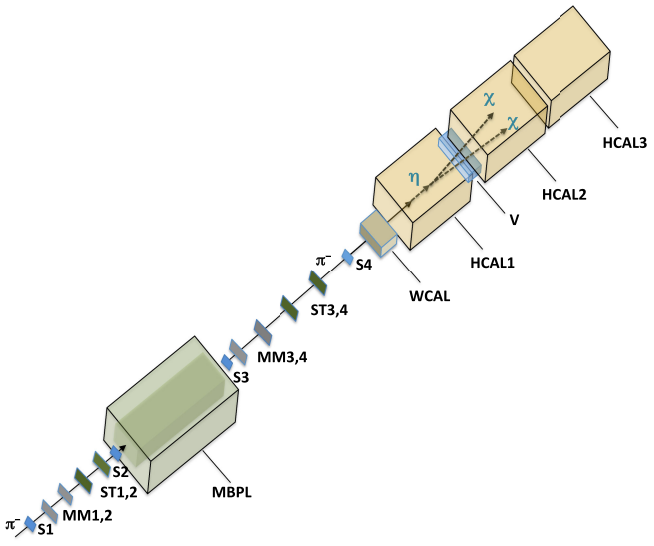

FIG. 2. Schematic illustration of the NA64h setup and of signal-like event.

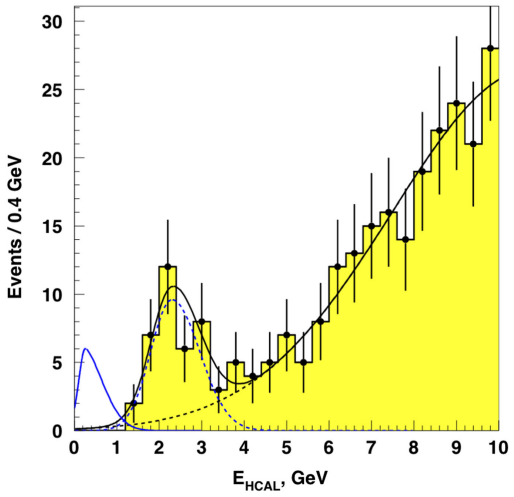

FIG. 3. The measured distribution of the total energy deposited in three HCAL modules (HCAL1 + HCAL2 + HCAL3) with signal selection cuts applied, i.e., for events with the energy deposited in Veto $E_{\rm VETO} \lesssim 2$ MeV. The expected total background contributions (solid black) are overlaid on the data (points) from the shaded area. The peak at ~2.5 GeV (dashed blue) corresponds to the background component due to backward muons from $K^- \to \mu^- \bar{\nu}_\mu$ decays, the smooth background above $\gtrsim$3 GeV is the energy deposited in the HCAL by poorly vetoed muons from $K^- \to \mu^- \bar{\nu}_\mu$ decaying forward. The shape of the expected signal distribution from the $\eta \to$ invisible decay (solid blue) is normalized to ten signal events. For the $\eta' \to$ invisible the signal shape is very similar.

with a total magnetic field of $\simeq$7 T · m and a low-material-budget tracker composed of a set of two upstream micromegas ($MM_{1,2}$) and two straw-tube chambers ($ST_{1,2}$), and two downstream MM_{3-4}, $ST_{3,4}$. Downstream, the setup is equipped with a tungsten electromagnetic calorimeter (WCAL) of $\simeq$10 radiation lengths (X_0) to reject low-energy electrons in the beam. The hadronic calorimeter (HCAL) is composed by three modules (HCAL1–3), for the measurement of the full energy $E_{\rm HCAL}$ deposited by the beam. Each HCAL module is a matrix of 3 × 3 cells assembled from Fe and Sc plates of $\simeq$7.5 nuclear interaction lengths (λ). The HCAL1 is followed by a high-efficiency veto counter (V) to enhance the rejection of events with hadronic secondaries produced in the π^-–nuclei interactions in the target.

The key point of the design is that the HCAL serves simultaneously as an active dump target composed mostly of Fe(26,52) nuclei, and a massive, hermetic detector absorbing all the secondaries from the reaction $\pi^- + {\rm Fe} \to$ anything, which occurs typically at the first λ of the HCAL1.

Our data sample of 2.93×10^9 pions on target was collected with the trigger requiring the HCAL energy $E_{\rm HCAL} \lesssim 20$ GeV. A GEANT4 [28,29] based Monte Carlo (MC) simulation package DMG4 [30,31] is used to study the performance of the detector, define the selection cuts, estimate the signal acceptance and background level. To maximize the signal or background ratio, the following selection criteria were used: (i) The incoming track must have momentum 50 ± 5 GeV and the deflected track angle should be within 3 mrad to reject events from the upstream π^- interactions. (ii) There should be no multiple hits in the $ST_{3,4}$ chambers to reject events with charged secondaries produced in the upstream beamline material. (iii) The WCAL energy should be within the range $\simeq$100–200 MeV expected from a a minimum ionizing particle (MIP). (iv) The HCAL energy deposit should be $\lesssim$20 GeV (trigger condition). (v) The VETO energy must satisfy $E_{\rm VETO} < 2$ MeV (~30% of the average MIP energy). The low energy part of the HCAL energy distribution from $\simeq 9.6 \times 10^5$ events satisfying these criteria, is shown in Fig. 3.

The signal events from the reaction (1) are expected to deposit no or small energy in the HCAL target. The latter can result from: (i) the HCAL noise and pileup events, measured directly with the random trigger; (ii) ionization losses of primary pion inside the target prior the pion interaction, defined from simulations and cross-checked with the energy deposited by punchthrough muons; and (iii) poorly reconstructed recoil neutrons or nuclear fragments resulting from the reaction (1). This contribution was simulated by using the measured differential cross sections $d\sigma/dt$ of the reaction (1) as a function of the momentum

TABLE I. Expected background for 2.93×10^9 pions on target.

Background source	Background, n_b
(i) Backward muons from $K_{2\mu}$ decay	0.08 ± 0.03
(ii) Energy loss from primary pion interactions	0.27 ± 0.1
(iii) Punchthrough leading n, K_L^0	< 0.01
Total n_b	0.35 ± 0.13

transfer t, assuming that the deposit from the nucleus break-up is small [32,33]. Finally, all the (i)–(iii) contributions were summed up defining the shape of the signal from the reaction (1), which is shown in Fig. 3.

The total background in the signal region $\lesssim$1 GeV has several components shown in Table I: (i) The main and most sophisticated background, peaking around ∼2.5 GeV as shown in Fig. 3, is from the $K^- \to \mu^- \bar{\nu}_\mu$ decay in flight after the magnet with the muon momentum directed backward, in the K^- rest frame, with respect to the beam momentum. The momentum of these muons is constrained by the geometrical acceptance of the S4 counter in the $2.2 < P_m u < 3.4$ GeV range, see Fig. 2 and most of them stop in the HCAL1 resulting in a broad peak as shown in Fig. 3. These low-energy decay muons penetrate the WCAL depositing energy via ionization and stop in the HCAL1 module with the energy deposition close to the signal region. Those muons from $K^- \to \mu^- \bar{\nu}_\mu$ decay that decay perpendicular to the K^- direction, typically escape detection as they do not trigger the S4 counter. The number of $K^- \to \mu^- \bar{\nu}_\mu$ decays is estimated from the simulations considering the beam composition measurements from [26]. (ii) The second bulk component includes events from the HCAL low-energy tail $E_{\mathrm{HCAL}} \lesssim 10$ GeV which deposited smaller energy due to the energy leak resulting from secondary $\pi, K \to e(\mu) + \bar{\nu}_e(\bar{\nu}_\mu)$ decays in the target and escaping neutrals. A small contribution also arises from $K^- \to \mu^- \bar{\nu}_\mu$ decays when the muon momentum in the rest frame of the kaon is in the forward direction. These muons can trigger the S4 counter with a momentum typically $P_\mu \gtrsim 10$ GeV with a lower energy tail due to the beam divergence and poor energy reconstruction. The Veto does not detect a small fraction of these muons ($\lesssim 10^{-3}$). This inefficiency was estimated from the measurements with the single muon punch-through in the HCAL. (iii) Punchthrough of leading neutral hadrons (n, K_L^0) from the π^- interactions in the target estimated from the direct measurements of punchthrough events as described in Ref. [34] is negligible. After applying the cuts, we expect mostly background events of type (i) and (ii) to remain in the analysis.

To obtain upper limits on the $\eta, \eta' \to$ invisible branching ratios, the analysis of events using the technique of limit setting based on the RooStats package [35] was performed. First, to define the optimal signal box, the expected signal shape and background level, efficiencies, and uncertainties were used for comparing sensitivities calculated as a function of the HCAL energy cut E_{cut}. The sensitivity was defined as an average expected limit calculated using the profile likelihood ratio method. To reduce uncertainties and the dependence on MC simulations, the expected number of background events n_b in the signal box was finally obtained directly from the data. The measured HCAL energy distribution was fitted to the sum of two functions $f_0 = f_1 + f_2$, where f_1 describing the backward decay muon peak and f_2 the second bulk event component, respectively, as depicted in Fig. 3. The shape of the extrapolation functions was taken from the analysis of the data and cross-checked with simulations by normalizing the peaking background component in the MC to the number of data events. The evaluation of n_b was obtained by extrapolating the function f_0 to the signal region. The systematic errors arising from the normalization and signal efficiency uncertainties were assessed by varying the fit functions. Finally, the candidate events were requested to have HCAL energy $E_{\mathrm{HCAL}} \lesssim 0.85$ GeV, thus, for the background extrapolation only energy deposition greater than this threshold in the active target is considered. The estimated background inside the signal region was 0.35 ± 0.13 events. After determining all the selection criteria and background levels, no event is found in the signal region.

The upper limits for $\mathrm{Br}(\eta^{(\prime)} \to \mathrm{invisible})$ are obtained from the 90% CL upper limit for the expected number of signal events, $n_{\eta^{(\prime)}}^{90\%}$ by applying the modified frequentist approach for confidence levels, considering the profile likelihood ratio as a test statistic [36–38]. The number of signal events $n_{\eta^{(\prime)}}$ from the $\eta^{(\prime)} \to$ invisible decay in the signal box is given by

$$n_{\eta^{(\prime)}} = n_\pi \epsilon_{tr} \epsilon_\pi \epsilon_{\eta^{(\prime)}} \frac{\sigma(\pi^-, \eta^{(\prime)})}{\sigma(\pi, \mathrm{tot})} \mathrm{Br}(\eta^{(\prime)} \to \mathrm{invisible}), \quad (2)$$

where n_π, ϵ_{tr}, and ϵ_π are, respectively, the number of incoming pions on target, the trigger efficiency for the signal events, and the efficiency for the incoming pion defined as a product of the pion track reconstruction efficiency (0.91 ± 0.012) and the probability for the pion to produce the MIP signal in the WCAL by passing it without interaction (0.52 ± 0.01). The ϵ_{tr} value was estimated from the measurements with a muon component in the beam, which produced events in the target with a MIP signal that is close to the signal event region. The ϵ_π value was extracted from the measurements with the pion beam. The signal acceptances ϵ_η and $\epsilon_{\eta'}$ were calculated by taking into account the shape of the η and η' signal distributions in the target for the given HCAL energy cut (0.85 GeV). The cross sections $\sigma(\pi^-, \eta^{(\prime)})$ of the reaction (1) were evaluated from the set of direct measurements of the charge exchange reactions on H, Li, C, Al, and Cu nuclei for the π^0, η, and η' final states for the beam energies up to 50 GeV [32,39–47] and found to be $\sigma(\pi^-, \eta) = 21.9 \pm 7.5$ μb and $\sigma(\pi^-, \eta') = 10.4 \pm 3.5$ μb for Fe nuclei at 50 GeV as described in [33]. The total cross-section for the 50 GeV pion absorption on Fe target, $\sigma(\pi, \mathrm{tot}) = 556 \pm 16$ mb was evaluated from the measurements performed for different target nuclei and a wide range of energies in Ref. [48]. The values of all variables from Eq. (2) are summarized in Table II together with their corresponding uncertainties, which include both statistical and systematic errors. Finally, the 90% CL

TABLE II. Summary of variables and their errors from Eq. (2).

Variable	Value and its error (in %)
n_π	$(2.93 \pm 0.06(2)) \times 10^9$
ϵ_{tr}	0.98 ± 0.02 (2)
ϵ_π	0.47 ± 0.01 (2.3)
ϵ_η	0.75 ± 0.023 (3)
$\epsilon_{\eta'}$	0.73 ± 0.022 (3)
$\sigma(\pi^-, \eta)$	21.9 ± 7.5 μb (34)
$\sigma(\pi^-, \eta')$	10.4 ± 3.5 μb (33)
$\sigma(\pi^-, \text{tot})$	554 ± 16 mb (2.9)

exclusion limits on $\eta, \eta' \to$ invisible decays,

$$\text{Br}(\eta \to \text{invisible}) < 1.1 \times 10^{-4}, \tag{3}$$

$$\text{Br}(\eta' \to \text{invisible}) < 2.1 \times 10^{-4}, \tag{4}$$

obtained by taking into account the estimated background and errors included in Eq. (2) are dominated by the uncertainty of ∼34% in the η and η' production cross sections.

In summary, the proof-of-concept search with NA64h places the first constraints on $\eta, \eta' \to$ invisible decays using charge exchange reaction as a source of η and η' mesons and missing energy as a powerful signal signature. Our limit of Eq. (3) is comparable, while the limit of Eq. (4) is more stringent by a factor of ≃3 compared to the current best limits set by BESIII [21]. These results demonstrate the effectiveness of our approach. Improving the beam quality by installing Cherenkov counters to suppress the kaon component, using a high-granularity active target, extending running times, and enhancing the background characterization are all concrete avenues to further improve the sensitivity in future searches. A significant improvement in the accuracy of the measurement of the cross section (1), compared to our current knowledge [33] would also reduce significantly the main systematic source of the measurement. The strategy could be to try to combine the search for $\eta^{(\prime)} \to$ invisible decays and measurements of the $\eta^{(\prime)} \to \gamma\gamma$ yield from the reaction (1) in the same setup. Finally, our method could also be used to search for leptophobic dark sectors in invisible decays of vector mesons [49,50].

Acknowledgments—We gratefully acknowledge discussions with V. Valuev, the support of the CERN management and staff, as well as contributions from HISKP, University of Bonn (Germany), ETH Zurich and SNSF Grants No. 186181, No. 186158, No. 197346, No. 216602 (Switzerland), ANID—Millennium Science Initiative Program—ICN2019 044 and Grants FONDECYT No. 1240216, No. 1240066, No. 3230806 (Chile), RyC-030551-I and PID2021-123955NA-100 and CNS2022-135850 funded by MCIN/AEI/FEDER, UE (Spain). This result is part of a project that has received funding from the European Research Council (ERC) under the European Union's Horizon 2020 research and innovation programme, Grant Agreement No. 947715 (POKER).

[1] R. L. Workman *et al.* (Particle Data Group), Prog. Theor. Exp. Phys. **2022**, 083C01 (2022).
[2] L. Arnellos, W. J. Marciano, and Z. Parsa, Nucl. Phys. **B196**, 365 (1982).
[3] D.-N. Gao, Phys. Rev. D **98**, 113006 (2018).
[4] L. Gan, B. Kubis, E. Passemar, and S. Tulin, Phys. Rep. **945**, 1 (2022).
[5] J. F. Kamenik and C. Smith, J. High Energy Phys. 03 (2012) 090.
[6] S. N. Gninenko, Phys. Rev. D **91**, 015004 (2015).
[7] S. N. Gninenko and N. V. Krasnikov, Phys. Rev. D **92**, 034009 (2015).
[8] S. N. Gninenko and N. V. Krasnikov, Mod. Phys. Lett. A **31**, 1650142 (2016).
[9] D. Barducci, M. Fabbrichesi, and E. Gabrielli, Phys. Rev. D **98**, 035049 (2018).
[10] M. Hostert, K. Kaneta, and M. Pospelov, Phys. Rev. D **102**, 055016 (2020).
[11] J. Elam *et al.* (REDTOP Collaboration), arXiv:2203.07651.
[12] C. Boehm and P. Fayet, Nucl. Phys. **B683**, 219 (2004); C. Boehm, D. Hooper, J. Silk, M. Casse, and J. Paul, Phys. Rev. Lett. **92**, 101301 (2004); P. Fayet, Phys. Rev. D **70**, 023514 (2004); **74**, 054034 (2006).
[13] B. McElrath, Phys. Rev. D **72**, 103508 (2005).
[14] L. Darme, S. A. R. Ellis, and T. You, J. High Energy Phys. 07 (2020) 053.
[15] B. Batell, P. deNiverville, D. McKeen, M. Pospelov, and A. Ritz, Phys. Rev. D **90**, 115014 (2014); B. Batell, A. Freitas, A. Ismail, and D. McKeen, Phys. Rev. D **100**, 095020 (2019).
[16] Y. Ema, F. Sala, and R. Sato, SciPost Phys. **10**, 072 (2021).
[17] T. Li, X.-D. Ma, and M. A. Schmidt, J. High Energy Phys. 07 (2020) 152.
[18] E. Cortina Gil *et al.* (NA62 Collaboration), J. High Energy Phys. 02 (2021) 201.
[19] M. Ablikim *et al.* (BES Collaboration), Phys. Rev. Lett. **97**, 202002 (2006).
[20] P. Naik *et al.* (CLEO Collaboration), Phys. Rev. Lett. **102**, 061801 (2009).
[21] M. Ablikim *et al.* (BESIII Collaboration), Phys. Rev. D **87**, 012009 (2013).
[22] M. Ablikim *et al.* (BESIII Collaboration), Chin. Phys. C **36**, 915 (2012).
[23] S. N. Gninenko, N. V. Krasnikov, and V. A. Matveev, Usp. Fiz. Nauk **191**, 1361 (2021).
[24] P. Crivelli, arXiv:2301.09905.
[25] See, for example, http://sba.web.cern.ch/sba/.
[26] Yu. M. Andreev *et al.* (NA64 Collaboration), Nucl. Instrum. Methods Phys. Res., Sect. A **1057**, 168776 (2023).
[27] D. Banerjee, P. Crivelli, and A. Rubbia, Adv. High Energy Phys. **2015**, 105730 (2015).
[28] S. Agostinelli *et al.* (GEANT4 Collaboration), Nucl. Instrum. Methods Phys. Res., Sect. A **506**, 250 (2003).
[29] J. Allison *et al.*, IEEE Trans. Nucl. Sci. **53**, 270 (2006).

[30] M. Bondi, A. Celentano, R. R. Dusaev, D. V. Kirpichnikov, M. M. Kirsanov, N. V. Krasnikov, L. Marsicano, and D. A. Shchukin, Comput. Phys. Commun. **269**, 108129 (2021).
[31] B. Banto Oberhauser, P. Bisio, A. Celentano, E. Depero, R. R. Dusaev, D. V. Kirpichnikov, M. M. Kirsanov, N. V. Krasnikov, A. Marini, L. Marsicano, L. Molina-Bueno, M. Mongillo, D. A. Shchukin, H. Sieber, and I. V. Voronchikhin, Comput. Phys. Commun. **300**, 109199 (2024).
[32] V. D. Apokin *et al.*, Sov. J. Nucl. Phys. **46**, 644 (1987).
[33] S. N. Gninenko, D. V. Kirpichnikov, S. Kuleshov, V. E. Lyubovitskij, and A. S. Zhevlakov, Phys. Rev. D **109**, 075021 (2024).
[34] D. Banerjee *et al.* (NA64 Collaboration), Phys. Rev. Lett. **125**, 081801 (2020).
[35] I. Antcheva *et al.*, Comput. Phys. Commun. **180**, 2499 (2009).
[36] T. Junk, Nucl. Instrum. Methods Phys. Res., Sect. A **434**, 435 (1999).
[37] G. Cowan, K. Cranmer, E. Gross, and O. Vitells, Eur. Phys. J. C **71**, 1 (2011).
[38] A. L. Read, J. Phys. G **28**, 2693 (2002).
[39] V. N. Bolotov, V. V. Isakov, V. A. Kachanov, D. B. Kakauridze, V. M. Kutjin, Yu. D. Prokoshkin, E. A. Razuvaev, V. G. Rybakov, V. K. Semenov, and V. A. Senko, Nucl. Phys. **B73**, 365 (1974).
[40] V. N. Bolotov, V. V. Isakov, V. A. Kachanov, D. B. Kakauridze, V. M. Kutjin, Yu. D. Prokoshkin, E. A. Razuvaev, V. G. Rybakov, V. K. Semenov, and V. A. Senko, Nucl. Phys. **B73**, 387 (1974).
[41] V. N. Bolotov, V. V. Isakov, V. A. Kachanov, D. B. Kakauridze, V. M. Kutjin, Yu. D. Prokoshkin, E. A. Razuvaev, and V. K. Semenov, Nucl. Phys. **B85**, 158 (1975).
[42] W. D. Apel *et al.*, Nucl. Phys. **B152**, 1 (1979).
[43] W. D. Apel *et al.*, Phys. Lett. **83B**, 131 (1979).
[44] V. Flaminlo *et al.*, Report No. CERN HERA 79-01, 1979.
[45] C. Daum *et al.*, Z. Phys. C **8**, 95 (1981).
[46] F. Binon *et al.*, Il Nuovo Cimento **64 A**, 89 (1981).
[47] V. D. Apokin *et al.*, Sov. J. Nucl. Phys. **35**, 219 (1982).
[48] A. S. Carroll *et al.*, Phys. Lett. **80B**, 319 (1979).
[49] P. Schuster, N. Toro, and K. Zhou, Phys. Rev. D **105**, 035036 (2022).
[50] A. S. Zhevlakov, D. V. Kirpichnikov, S. N. Gninenko, S. Kuleshov, and V. E. Lyubovitskij, Phys. Rev. D **108**, 115005 (2023).

Correction: A typographical error was introduced during the production cycle in the Collaboration name appearing below the author list and has been fixed.